climate

MDPI

Article

Hydrologic Alterations Predicted by Seasonally-Consistent Subset Ensembles of General Circulation Models

Aleksey Y. Sheshukov [1,*] and Kyle R. Douglas-Mankin [2]

[1] Department of Biological and Agricultural Engineering, Kansas State University, Manhattan, KS 66506, USA
[2] New Mexico Water Science Center, U.S. Geological Survey, Albuquerque, NM 87113, USA; krdmankin@gmail.com
* Correspondence: ashesh@ksu.edu; Tel.: +1-785-532-5418

Academic Editors: Daniele Bocchiola, Claudio Cassardo and Guglielmina Diolaiuti
Received: 17 May 2017; Accepted: 21 June 2017; Published: 26 June 2017

Abstract: Future climate forcing data at the temporal and spatial scales needed to drive hydrologic models are not readily available. Simple methods to derive these data from historical data or General Circulation Model (GCM) results may not adequately capture future hydrological variability. This study assessed streamflow response to daily future climate forcing data produced by a new method using subsets of multi-model GCM ensembles for the mid-21st century period in northeast Kansas. Daily timeseries of precipitation and temperature were developed for six future climate scenarios: stationary, uniform 10% changes in precipitation; shifts based on a 15-GCM ensemble-mean; and shifts based on three seasonally-consistent subsets of GCMs representing Spring–Summer combinations that were wetter or drier than the historical period. The analysis of daily streamflow and hydrologic index statistics were conducted. Stationary 10% precipitation shifts generally bounded the monthly mean streamflow projections of the other scenarios, and the 15-GCM ensemble-mean captured non-stationary effects of annual and seasonal hydrological response, but did not identify important intra-annual shifts in drought and flood characteristics. The seasonally-consistent subset ensembles produced a range of distinct monthly streamflow trends, particularly for extreme low-flow and high-flow events. Meaningful water management and planning for the future will require hydrological impact simulations that reflect the range of possible future climates. Use of GCM ensemble-mean climate forcing data without consideration of the range of seasonal patterns among models was demonstrated to remove important seasonal hydrologic patterns that were retained in the subset ensemble-mean approach.

Keywords: climate change; general circulation models; weather generator; hydrology; SWAT; IHA

1. Introduction

Scientific centers around the world have developed General Circulation Models (GCMs) for prediction of future climate trends. Each GCM accounts for sea, atmosphere, and land interactions and simulates climate projections on grids with resolution from 2500 km^2 to 200,000 km^2 [1,2]. The results of GCMs carry a certain degree of uncertainty associated with different modeling algorithms, physical model assumptions, temporal and spatial resolution, and implementation of emission-scenario assumptions [3–5]. Since the resolution of GCMs is generally coarse for adequate estimation of the impacts of climate projections on hydrologic processes in a watershed, and in consideration of known GCM output uncertainty, methods to downscale or bias-correct the model outputs have been developed [6–9]. One family of downscaling methods involves a statistical approach of applying smaller-scale climatic observations to bias-correct the larger-scale GCM data [7,10,11]. Stochastic

weather generators can be used to generate numerous instances of future daily climate variables by adjusting historical weather patterns based on GCM projections for mid-21st or late-21st century periods [11–14].

A number of studies have simulated hydrologic responses in watersheds around the world as a result of weather predictions by GCMs [15–17] or shifts in seasonal precipitation and temperature [13,16,18,19]. The increased temperature and changing patterns in precipitation intensity, duration, and timing can substantially affect streamflow, groundwater recharge, crop yields, and other environmental variables in the future [20,21]. Brunsell et al. [22] predicted significant seasonal trends of temperature (+0.04 °C/yr) and precipitation (+0.075 mm/yr in spring, +0.024 mm/year in winter, −0.06 mm/yr in summer, and +0.04 mm/yr in fall) for the intermediate emission path (A1B scenario [2]) in the 21st century in Kansas that could fundamentally change hydrologic processes and significantly impact industry and agricultural production in the region [11,17,22,23].

The use of multiple GCMs is widely recognized as an acceptable method in representing future climate projections because of uncertainty in model predictions associated with individual GCMs, with many studies using the ensemble-mean approach. However, acquiring, processing, and downscaling of GCM data outputs is a laborious process. In addition, the bias generated by assumptions and specifics of an individual GCM selected for GCM ensemble can affect the outcomes of the research.

Therefore, the main goal of this study was to evaluate the effects of two common methods, stationary, uniform shifts from historical climate patterns and shifts based on multi-model ensembles of GCMs, and a new method using seasonally-consistent subset ensembles of GCMs, on alteration of hydrologic regimes from late-20th century to mid-21st century predictions. The specific objectives were to (1) demonstrate and assess a method to identify subsets of GCMs based on similar projected seasonal patterns in northeast Kansas, (2) analyze the impacts on monthly streamflow, and (3) evaluate the climate impacts on hydrologic characteristics of drought and floods that affect natural habitat and stream ecosystems.

2. Materials and Methods

2.1. Study Area

The Soldier Creek watershed is a 769 km^2 10-digit Hydrologic Unit Code 1027010209 watershed in Nemaha, Jackson and Shawnee counties of northeast Kansas, USA (Figure 1). Land use, comprised of pastureland (42%), rangeland (23%), and cropland (19%), was relatively unchanged since the 1960s after channelization of the lower portion of Soldier Creek close to the city of Topeka [24]. Most cropland and forestland (8%) are located in areas adjacent to streams and creeks. The landscape relief is gentle with median slope of 2.7%. Soils are generally silt loam and clay loam with mean permeability of 5 mm/h and hydrologic soil groups of mainly B (53% of area) and D (35%). The outlet of the watershed is located at the United States Geological Survey (USGS) streamflow gaging station 06889500 near the city of Topeka, Kansas [25].

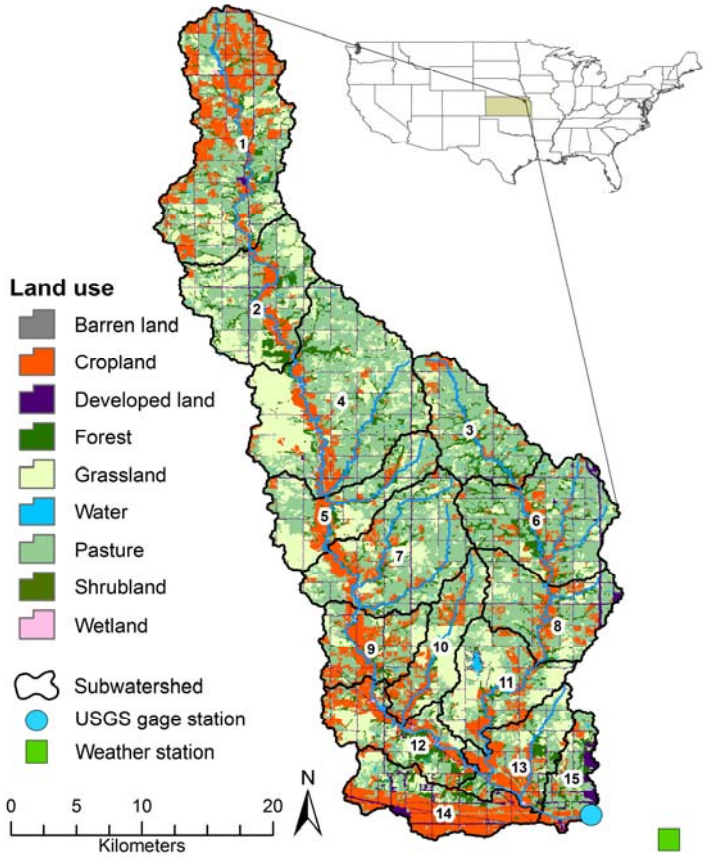

Figure 1. Soldier Creek watershed in northeast Kansas, USA, showing watershed boundaries, subwatersheds, weather station, and streamflow gaging station.

2.2. Hydrologic Model

The Soil and Water Assessment Tool (SWAT, ver. 2009, http://swat.tamu.edu) [26,27] was employed to simulate hydrological response to past, present, and future climate scenarios. SWAT is a physically-based continuous watershed simulation model that incorporates a set of physically and empirically based equations to simulate hydrologic and water quality processes on a daily scale [28,29]. SWAT has been widely used for hydrologic predictions at watershed scales imposed by future climate scenarios from downscaled and bias-corrected GCMs [11,20,29–32]. The details of the SWAT individual simulation components can be found at Neitsch et al. [27].

For geospatial division of a watershed, SWAT delineates a watershed into subwatersheds, creates a stream network, and prepares subareas, called hydrologic response units (HRUs), having homogeneous properties of slope, land use, and soil type within each subwatershed. Within each HRU, SWAT calculates daily water-budget components based on daily precipitation input, infiltration, surface runoff, evapotranspiration (ET), groundwater recharge, and return flow.

For Soldier Creek watershed, fifteen 12-digit Hydrologic Unit Code subwatersheds ranging from 5000 to 20,000 ha were delineated from 30-m digital elevation model [33], and 878 HRUs were created using NLCD land use/land cover data [33,34] and STATSGO2 soil data [33]. Land management and farming operations were based on data from KSU extension publications, watershed reports [35], and communications with watershed extension specialists. Daily precipitation and minimum and maximum temperature from was taken from the cooperative weather station 147007 (Figure 1) located at the Topeka airport [36] for the late 20th century period from 1980 to 1999.

The SWAT model was carefully calibrated using daily streamflow at the watershed outlet from USGS gauge station 06889500 [25] for the period of 1980 to 1999. Eleven model parameters

related to surface and groundwater hydrology, plant growth, and snowmelt dynamics were adjusted iteratively until acceptable model-performance statistics were reached. The values of coefficient of determination (R^2; 0.56 for daily, 0.74 for monthly, and 0.88 for annual statistics), Nash-Sutcliffe efficiency (NSE; 0.56, 0.73, 0.84), and percent bias (pBias; 5.69, 5.78, 5.69) were rated good (R^2, NSE) to very good (pBias) according to criteria proposed by Moriasi et al. [37]. The detailed calibration procedure, adjusted parameter values, calibration statistics, and water balance components can be found in [11,38]. The calibrated model represented watershed conditions for the historical period well and was deemed suitable for this study.

2.3. Hydrologic Indexes

The Indicators of Hydrologic Alteration, IHA, [39] software was used to evaluate intra-annual streamflow characteristics during historical and projected periods of simulations. Nine hydrologic indexes were selected for the analysis: mean annual streamflow, low-flow pulse count and duration, small-flood peak, duration, and frequency, and large-flood peak, duration, and frequency. Low-flow indexes represent drought characteristics. Large-flood indexes show extreme flow conditions of streams overtopping banks, while small-flood indexes represent near-bank-full conditions. Low-flow pulse threshold for streamflow is defined by the annual mean flow minus one standard deviation. Low-flow pulse count is the number of times per year the daily streamflow falls below the threshold, and low-flow pulse duration is the mean number of days per year below the threshold per occurrence, as discussed. Small floods are continuous periods of time when daily streamflow values exceed the annual mean flow plus one standard deviation and represent events with 2-year return interval. Large floods are similar to small floods but for events with 10-year return interval or higher. The duration and frequency of small- and large-flood events are obtained in continuous days and number of events per year.

2.4. Climate Data Processing

General Circulation Models (GCM) have been developed by a number of research teams to simulate atmospheric, land, and sea interactions as forced by probable future emissions scenarios [2]. Among the Coupled Model Intercomparison Project Phase 3 (CMIP3) report emission scenarios, the A2 scenario (high economic growth, low technology development, high population growth), generally referred to as a high-emission scenario, was considered to result in extreme environmental impacts [2] and was selected for this study.

A total of 24 GCMs were available in the IPCC online datacenter [1]. From these, 15 GCMs from 13 research teams and 9 countries (Table 1) were selected for this study. Their selection was based on availability of data for both the historical period of the second half of the 20th century (1961 to 1990) and mid-21st century projection period (2046 to 2065). No other specific considerations on model accuracy were made for GCM selection. The selected GCMs were developed for different spatial resolutions with grid-cells varying from 18,000 km^2 to close to 200,000 km^2. The coarsest grids were in the NASA GISS-ER and INM CM3.0 models, and the finest grid was in the NCAR CCSM3 model.

For each GCM, an individual rectangular grid-cell with center point closest to the centroid of Soldier Creek watershed was selected (Table 1; Figure 2). For all 15 GCMs, monthly precipitation and temperature dataseries were acquired for the selected grid-cells for two studied periods (1961–1990 and 2046–2065) from the IPCC online datacenter [1]. Although, a single grid-cell approach may seem to provide a certain disadvantage in representing projected weather within a watershed as compared to including interpolation from the nearest grid-cells, the coarse resolution of the GCMs themselves can be viewed as a major factor for inaccuracy [7,13]. To minimize the downscaling bias, GCM data were bias-corrected on historical data from a land-based weather station.

Table 1. 15 CMIP3 general circulation models [1], grid-cell resolution (degrees) and center point (latitude, longitude).

	Model		Grid Cell	
	Name	**Country**	**Center Point**	**Resolution**
1	CNRM CM3	France	40.45, 264.38	2.80 × 2.80
2	CSIRO Mk3.0	Australia	40.09, 264.38	1.875 × 1.875
3	MHP ECHOG	Germany, Korea	38.94, 262.50	3.75 × 3.75
4	GFDL CM2	U.S.A.	39.00, 263.75	2.00 × 2.50
5	GFDL CM2.1	U.S.A.	39.22, 263.75	2.00 × 2.50
6	NASA GISS-ER	U.S.A.	37.58, 262.50	4.00 × 5.00
7	UKMO HadCM3	U.K.	40.00, 262.50	2.75 × 3.75
8	UKMO HadGEM1	U.K.	38.75, 264.38	1.25 × 1.875
9	INM CM3.0	Russia	40.00, 265.00	4.00 × 5.00
10	IPSL CM4	France	39.30, 262.50	2.50 × 3.75
11	NIES MIROC 3.2medres	Japan	40.45, 264.38	2.80 × 2.80
12	MPI-OM ECHAM5	Germany	38.23, 264.38	2.80 × 2.80
13	MRI CGCM 2.3.2	Japan	40.45, 264.38	2.80 × 2.80
14	NCAR CCSM3	U.S.A.	39.91, 264.38	1.40 × 1.40
15	NCAR PCM	U.S.A.	40.45, 264.38	2.80 × 2.80

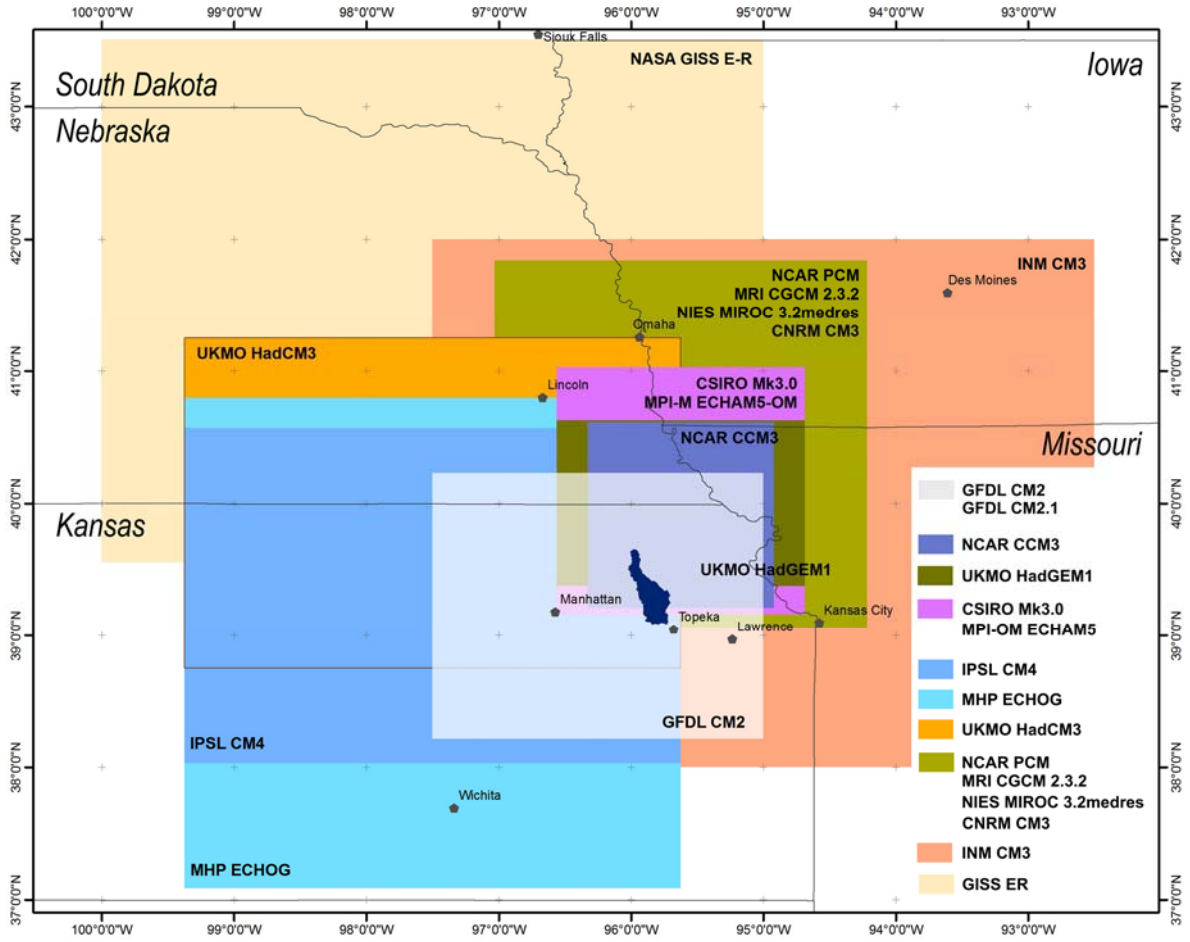

Figure 2. Single grid-cells of 15 General Circulation Models (GCMs) (see Table 1) used for climate data analysis of the Soldier Creek watershed in northeast Kansas.

In hydrologic simulations with SWAT, daily climate data are required as model inputs. To produce daily input data, a stochastic weather generator (Weather Input for Nonpoint Data Simulation; WINDS) was employed. WINDS used a two-step procedure [40]. First, it calculated daily statistics (mean, standard deviation) of the observed minimum and maximum temperature and precipitation at the Topeka airport weather station (Figure 1) for the historical period of 1961 to 1990. WINDS represented the statistics of each climate variable by cosine functions with three harmonics and seven coefficients [41]. The coefficients were adjusted to fit the observed dataseries with R^2 of 0.99 for mean and 0.94 for standard deviation of temperature; and R^2 of 0.95 (mean) and 0.89 (standard deviation) for precipitation. This statistics were used as a baseline for stochastic generation of daily weather timeseries. Second, WINDS applied a first-order autoregressive model within a statistical framework of Markov processes to generate daily values of non-precipitation variables. For precipitation, WINDS utilized a first-order, two-state Markov chain process based on the transitional probability of a wet day given that the previous day was wet (wet-wet) and given that the previous day was dry (dry-wet) to generate discrete 24-h precipitation events. This basic approach allowed generation of hundreds of years of daily weather data that were, on average, statistically representative of the studied period. Readers are referred to Wilson et al. [40] for complete details of the weather generation procedure in WINDS.

In order to use a weather generator for temporal downscaling of future monthly GCM dataset to the daily scale, a modification to WINDS was implemented. A normalizing factor was calculated for general statistics of means and standard deviation based on the differences between the actual dataset at the Topeka airport station, GCM historical 20th century period, and GCM mid-21st century projection period (Table 2). These differences were applied to normalized climate variables before the second step of the WINDS procedure was conducted for baseline and future daily weather dataset generation. In the utilized approach, each day of the year was simulated hundreds of times, thus providing enough data points for the output statistics.

The details of the downscaling technique are discussed in [11,42]. This approach represents a variant of post-processing bias-correction with the use of a stochastic weather generator and the change-factor method [43,44]. This method is efficient in generating weather timeseries for future projections, but constrained by the assumption that the weather cumulative distribution function retains properties of the historical dataset. The uncertainty associated with probabilities of the frequency and timing of extreme events in the future that are not fully represented in large-scale GCMs can have a strong effect on future model predictions. This can be alleviated by regional-scale models that better preserve local climate features. Further development of this topic is beyond the scope of this study.

2.5. Future Scenarios

All future climate scenarios were developed using the downscaling procedure outlined above. The normalizing factors that account for monthly adjustments in precipitation and temperature based on the differences in GCM predictions for late-20th century (1961 to 1990) and mid-21st century (2046 to 2065) were calculated for each GCM and applied to the WINDS stochastic generating procedure to produce daily time series that were input into the SWAT model. Based on the adjustments, four main sets of future climate scenarios were developed in this study: baseline, uniform shifts, ensemble mean shifts, and seasonal shifts. The values of precipitation and temperature adjustments used in all scenarios are presented in Table 2.

Table 2. Monthly mean precipitation (P, mm) and temperature (T, °C) for observed weather at the Topeka airport weather station 147007 (1980–2000), and weather adjustments (ΔP, ΔT) from late-20th century historical period (1961–1990) to mid-21st century projection (2046−2065, + indicates increase in future) for six climate change scenarios: 1a, 10% increase in precipitation; 1b, 10% decrease in precipitation; 2, ensemble means of 15 GCMs; 3ww, ensemble means of 4 GCMs with wetter spring and wetter summer; 3dd, ensemble means of 4 GCMs with drier spring and drier summer; 3wd, ensemble means of 6 GCMs with wetter spring and drier summer.

Scenario	Observed		1a	1b	2		3ww		3dd		3wd	
	P	T	ΔP	ΔP	ΔP	ΔT *	ΔP	ΔT	ΔP	ΔT	ΔP	ΔT
Jan	24	−2.6	2.4	−2.4	4.8	2.6	−0.2	2.8	0.4	2.4	7.0	2.8
Feb	23	0.5	2.3	−2.3	3.0	2.8	1.5	3.2	0.9	3.4	4.5	2.7
Mar	62	6.8	6.2	−6.2	4.2	2.8	6.7	2.6	2.8	3.4	7.0	2.9
Apr	81	12.7	8.1	−8.1	2.1	2.4	5.8	2.1	−13.1	3.1	7.7	2.6
May	124	18.1	12.4	−12.4	10.3	2.5	17.7	2.9	−7.7	2.9	19.8	2.5
Jun	139	23.3	13.9	−13.9	−8.3	3.0	12.5	2.7	−18.6	3.8	−18.8	3.1
Jul	93	26.0	9.3	−9.3	−12.3	3.5	13.4	2.6	−14.0	3.7	−28.6	4.6
Aug	87	24.9	8.7	−8.7	−7.3	4.0	16.1	2.9	−17.1	4.2	−18.1	5.4
Sep	116	20.2	11.6	−11.6	−4.1	3.8	11.9	3.1	−13.4	4.6	−6.2	4.2
Oct	76	13.6	7.6	−7.6	3.0	3.0	−5.0	3.7	14.8	3.3	−0.3	2.7
Nov	48	6.2	4.8	−4.8	2.8	2.7	−2.0	2.8	4.7	3.1	4.0	2.9
Dec	32	−0.5	3.2	−3.2	4.1	2.9	5.4	2.7	7.1	2.8	3.5	3.2
Average	**75**	**9.4**	**7.5**	**−7.5**	**0.2**	**3.0**	**7.0**	**2.8**	**−4.4**	**3.4**	**−1.5**	**3.3**

* Also applies to Scenarios 1a and 1b.

2.5.1. Baseline Scenario

The baseline scenario for the mid-21st century assumes no monthly changes in future temperature and precipitation from the late-20th century historical dataset [11,13,14,45]. The normalizing factor was assumed to be equal to unity. This baseline scenario considers unchanged future, and was used as control for comparison with the other scenarios.

2.5.2. Group 1 Scenarios: Uniform Shifts

Two scenarios in this group apply uniform changes in precipitation for all months, thus the normalizing factor is constant across all months. Scenario 1a assumes precipitation increase by 10%, while Scenario 1b applies a 10% decrease (Table 2). Monthly temperature was assumed to adjust according to ensemble means from 15 GCMs, as described in Scenario 2 below. Using the same temperature adjustment factors allowed a direct comparison of the simple ±10% precipitation shifts (e.g., [21]) to the ensemble mean approach of simulating hydrologic impacts of climate change.

2.5.3. Group 2 Scenario: Ensemble Mean Shifts

In Scenario 2, monthly means of the ensemble of 15 GCMs were used for both temperature and precipitation adjustments. Figure 3 shows quantiles and ranges of monthly precipitation (Figure 3a) and temperature (Figure 3b) adjustments that were used in defining the values of the normalizing factor, while Table 2 presents the means. Predictions by the ensemble of 15 GCMs showed the greatest range of monthly precipitation for summer months of June, July, and August, up to a range of 100 mm, and smallest range for winter to early spring months of December, January, February, and March. This climate scenario showed an increase in precipitation in spring (March, April, May), fall (September, October, November) and winter (December, January, February), and a decrease in precipitation during summer (June, July, August). The mean change in monthly temperature varied from 2 to 4 °C for all months, with the smallest range in May and largest range in August.

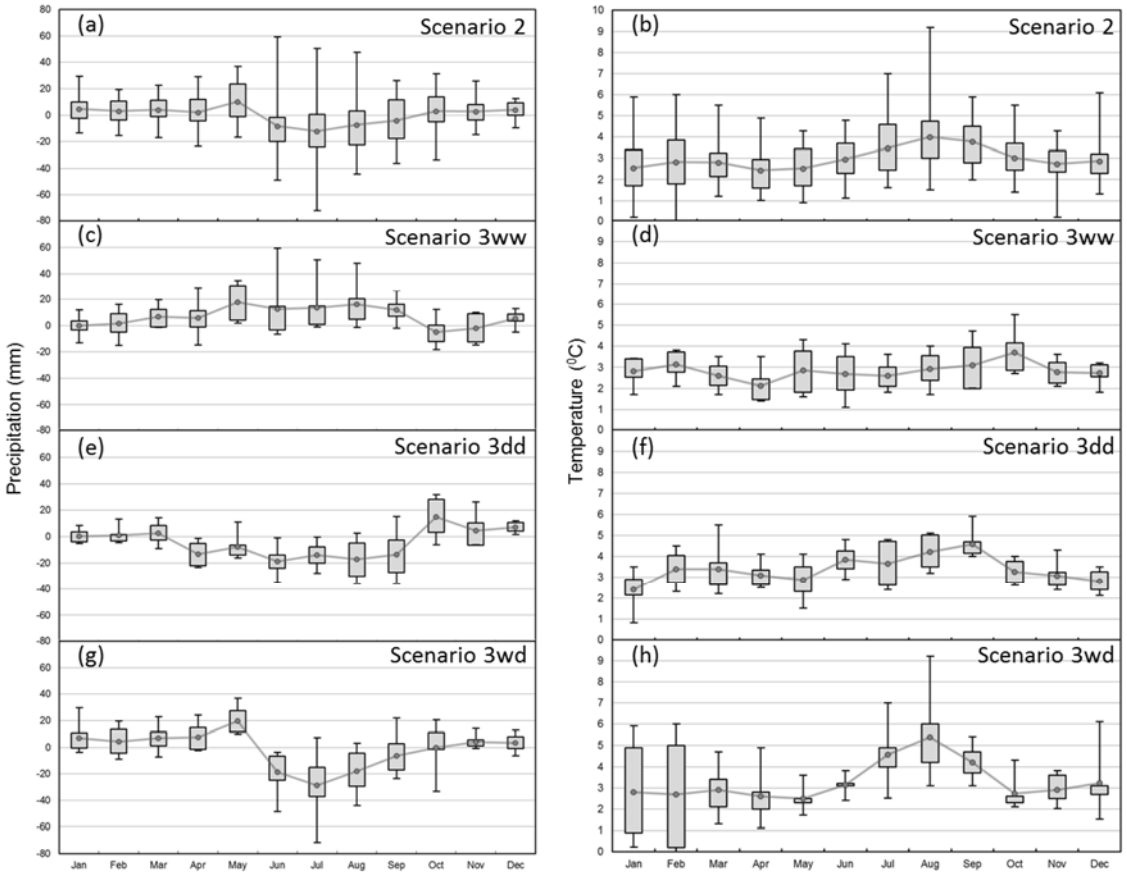

Figure 3. Changes in monthly precipitation (left) and temperature (right) from mid-21st century to late 20th century periods (+ indicates increase in future) for GCMs included in Scenarios 2 (**a**,**b**; n = 15), 3ww (**c**,**d**; n = 4), 3dd (**e**,**f**; n = 4), and 3wd (**g**,**h**; n = 6). Boxes show 25th and 75th quantiles, whiskers show maximums and minimums, and the solid line connects mean values.

2.5.4. Group 3 Scenarios: Seasonal Shifts

Three scenarios in this group were designed to represent different seasonal trends found in mid-21st century projections by 15 GCMs. The projections showed a consistent positive trend for temperature in all months while precipitation exhibited distinct seasonal increasing or decreasing trends for spring (March, April, May) and summer (June, July, August) that differed among GCMs. The trends in fall and winter were generally positive for all models, thus were not included in the seasonal analysis.

Table 3 presents a summary of seasonal analysis of 15 GCMs. The letter "w" indicates positive adjustment in precipitation (wetter future conditions), whereas the letter "d" is used for negative adjustments (drier future conditions). Three distinct trends in future spring–summer pairs were identified by 4 or more of the 14 GCMs: w–w, d–d, and w–d. One model (MPI-M CHAM5-OM) produced a spring–summer pairing (d-w) that was not replicated by any of the other 14 GCMs, and, therefore, was not considered further. Scenario 3ww contained 4 models with the w-w trend (CSIRO Mk3.0, CONS ECHOG, MRI CGCM2.3.2, NRAR CCSM3), Scenario 3dd consisted of 4 GCMs with the d-d trend (CNRM CM3, UKMO HadCM3, IPSL CM4, NIES MIROC3.2medres), and Scenario 3wd contained 6 models with the w-d trend (GFDL CM2, CFDL CM2.1, GISS E-R, UKMO HadGEM1, INM CM3.0, NCAR PCM).

Table 3. Seasonal analysis of precipitation changes in 15 GCMs from late 20th century to mid-21st century periods. Letter "d" represents a drier future and letter "w" represents a wetter future trend.

	MPI-M ECHAM5-OM	**CNRM CM3**	**IPSL CM4**	**NIES MIROC3.2 Medres**	**UKMO HadCM3**	**GFDL CM2**	**CFDL CM2.1**	**GISS E-R**	**UKMO HadGEM1**	**INM CM3.0**	**NCAR PCM**	**CSIRO Mk3.0**	**CONS ECHOG**	**MRI CGCM2.3.2**	**NRAR CCSM3**
Spring	d	d	d	d	d	w	w	w	w	w	w	w	w	w	w
Summer	w	d	d	d	d	d	d	d	d	d	d	w	w	w	w
Scenario	**-**	**3dd**	**3dd**	**3dd**	**3dd**	**3wd**	**3wd**	**3wd**	**3wd**	**3wd**	**3wd**	**3ww**	**3ww**	**3ww**	**3ww**

The quantiles and ranges of monthly precipitation for Scenarios 3ww, 3dd, and 3wd are shown in Figure 3c–h. All seasonal scenarios exhibited smaller variations in monthly adjustments than in Scenario 2, due to analyzing specific subsets of GCMs with greater seasonal consistency, particularly in Scenarios 3dd and 3ww with similar precipitation shifts in spring and summer. For Scenario 3ww, monthly precipitation exhibits substantial increase not only during spring and summer, but also in fall and winter. Scenario 3dd exhibited a decrease in precipitation in spring and summer, followed by an increase in precipitation in the late fall and early winter. This scenario produced the largest annual precipitation decrease out of all set 3 scenarios. Scenario 3wd was similar in its impact to Scenario 2, as it caused an increase in monthly precipitation in spring and a decrease in summer, with little net effect on the average annual precipitation.

The ensemble mean approach (Scenario 2) benefited from including multiple GCMs, but it also reduced the representation of seasonal precipitation variability by averaging GCMs that had opposite seasonal trends. The Group 3 scenarios retained the differences in seasonal precipitation from the different GCMs while also benefiting from including multiple GCMs with similar seasonal representations in each subset ensemble (3ww, 3dd, and 3wd). This seasonal precipitation variability should allow Group 3 scenarios to capture a range of projected future conditions that are masked by the typical ensemble mean approach of the Group 2 scenario.

2.5.5. Future Scenario Analysis

Daily streamflow was simulated with the SWAT model of the Soldier Creek watershed for 6 climate-change scenarios and a baseline (no change) scenario. Each scenario was represented in SWAT by different inputs of daily precipitation and minimum and maximum temperature timeseries generated with WINDS according to the downscaling procedure described above. SWAT model outputs included daily streamflow, water yield, infiltration, ET, baseflow, and other water budget components in each subwatershed. SWAT-simulated streamflow at the watershed outlet of USGS gaging station 06889500 was analyzed for annual and seasonal statistics, flow exceedance probability, and drought and extreme-event hydrological characteristics. Streamflows for future climate scenarios from groups 1, 2, and 3 were compared with baseline-scenario streamflow to determine the hydrological alterations caused by future climate projections. The IHA software was used for computing the indices of hydrologic alteration.

3. Results

3.1. Streamflow Analysis

The Baseline scenario (2046 to 2065) produced monthly streamflow with low flows in the winter and bi-modal peaks in May–June and October (Figure 4), which resulted from a bi-modal monthly precipitation pattern with peaks in May–June and September (Table 2). The one-month delay of streamflow peaks following the months of high precipitation presents a normal delay of about 30 days in baseflow contribution in northeast Kansas (see delay factor GW_DELAY in SWAT model [11]). All other scenarios will be discussed relative to this Baseline scenario.

Annual streamflow for the two scenarios of group 1 increased by an average of 1.1 m^3/s (+24%) for Scenario 1a or decreased by 1.5 m^3/s (−33%) for Scenario 1b (Table 4) relative to Baseline. The annual decrease for Scenario 1b was greater in magnitude than the increase for Scenario 1a due to the reinforcing impacts of decreased precipitation and increased temperature (which drives increased ET), both of which reduce net precipitation (precipitation minus ET) and streamflow.

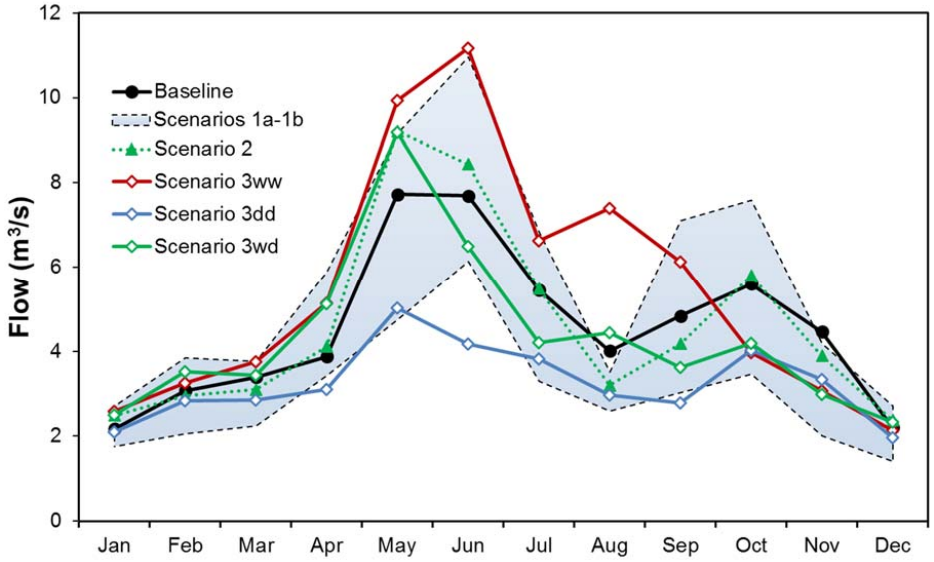

Figure 4. Monthly average streamflow (2046 to 2065) for the baseline and six future climate scenarios.

Table 4. Nine hydrologic indexes calculated from SWAT-simulated daily streamflow for the baseline and six future climate scenarios for the mid-21st century projection (2046–2065). The percentage in brackets shows change from Baseline.

	Baseline	1a	1b	2	3ww	3dd	3wd
Mean Annual Flow (m^3/s)	4.5	5.6 (24%)	3.0 (−33%)	4.6 (2%)	5.4 (20%)	3.2 (−29%)	4.3 (−4%)
Low-flow Pulse Count (#)	6.0	4.1 (−32%)	8.3 (38%)	6.7 (12%)	4.0 (−33%)	7.8 (30%)	7.0 (17%)
Low-flow Pulse Duration (days)	16.0	13.4 (−16%)	19.8 (24%)	14.7 (−8%)	17.2 (8%)	16.8 (5%)	16.3 (2%)
Small Flood Peak (m^3/s)	435	444 (2%)	456 (5%)	448 (3%)	421 (−3%)	371 (−15%)	462 (6%)
Small Flood Duration (days)	61.7	74.2 (20%)	29.4 (−52%)	59.8 (−3%)	57.5 (−7%)	31.4 (−49%)	62.4 (1%)
Small Flood Frequency (#/yr)	0.20	0.20 (0%)	0.10 (−50%)	0.20 (0%)	0.20 (0%)	0.05 (−75%)	0.14 (−30%)
Large Flood Peak (m^3/s)	777	838 (8%)	821 (6%)	862 (11%)	1294 (66%)	972 (25%)	1211 (56%)
Large Flood Duration (days)	61.4	69.2 (13%)	35.3 (−43%)	57.6 (−6%)	51.8 (−16%)	41.4 (−33%)	55.9 (−9%)
Large Flood Frequency (#/yr)	0.10	0.10 (0%)	0.10 (0%)	0.10 (0%)	0.04 (−60%)	0.05 (−50%)	0.11 (10%)

At a monthly resolution (Figure 4), the 10% shift in precipitation combined with the overall increase in ET resulting from the 2.4 to 4.0 °C increase in temperature to affect streamflow predictably across the 12 months of the year. For example, streamflow in August decreased for Scenario 1a relative to Baseline largely because the 10% increase in precipitation did not offset the +4.0 °C temperature-induced increase in ET. Also, baseflow delay can have a cumulative effect on streamflow. For example, whereas Baseline streamflow was similar in May and June, streamflow in Scenario 1a was greater in June resulting from excessive rainfall events in May that contributed to streamflow via lagged baseflow. For Scenario 1b, increased temperature during summer months decreased soil moisture and ET rates, thus contributing to larger decline of runoff and baseflow and, as a result, a negative effect on streamflow.

Monthly streamflow hydrographs of uniform-shift Scenarios 1a and 1b generally bounded the streamflow projections of the other scenarios (Figure 4). Although important seasonal interactions may be over-simplified, the ±10% precipitation scenarios are easy for modelers to develop from historical precipitation data sets, are easy to explain to stakeholders, and provide a reasonable range of monthly streamflow responses in this climatologic region.

Streamflows of the ensemble-mean-shift Scenario 2 generally fell within the range of Scenarios 1a and 1b. An important difference in streamflow pattern was evident in spring; Scenario 2 first increased more rapidly than Scenarios 1a and 1b from April to May and then declined in June, in contrast to Scenarios 1a and 1b, which both increased from May to June. The spring rainfall period is a critical time for precipitation in prairie and agroecosystems in the Great Plains, so these differences would be

expected to have important ramifications on prairie productivity and crop production [46]. Although Scenarios 1a and 1b may be simpler to generate, Scenario 2 may provide a more relevant representation of the seasonal precipitation patterns forecast by GCMs for the mid-21st century future period.

Monthly streamflow for Scenario 3ww generally followed Scenario 1a (+10% precipitation) from January through July. A string of wetter summer months led to substantially more streamflow than both Scenario 1a and Baseline in August, and less precipitation and elevated temperatures in fall months led to substantially less streamflow than both Scenario 1a and Baseline in October and November.

Scenario 3dd monthly streamflow generally followed Scenario 1b (–10% precipitation) in late spring (April–May) and late summer to early fall (July–September), reflecting the decreased spring and summer precipitation. However, the combination of less precipitation and greater temperature in June and September resulted in Scenario 3dd streamflow falling below Scenario 1b for those two months.

Scenario 3wd represented a hybrid of the other group 3 hydrographs, with similarities resulting from a similarly wet spring to Scenario 3ww and similarly dry summer to Scenario 3dd. Scenario 3wd had a very similar monthly pattern to Scenario 3ww from mid-fall through spring (October–December, January–May) but demonstrated rapidly declining streamflow in June and July, approaching Scenario 3dd in late summer (July).

The flow exceedance probability curves (Figure 5) provide a slightly different perspective on the streamflow impacts of the scenarios. There was very close agreement between Baseline and Scenario 2 and between Scenario 3ww and Scenario 1a throughout the entire range of probabilities in the exceedance curve. Scenario 3wd flows were slightly less than Baseline throughout the entire regime, and Scenario 3dd flows were substantially less than Baseline, converging with Scenario 3wd above the 90% exceedance level. Again, Scenarios 1a and 1b encompassed the range of streamflows simulated for the other scenarios.

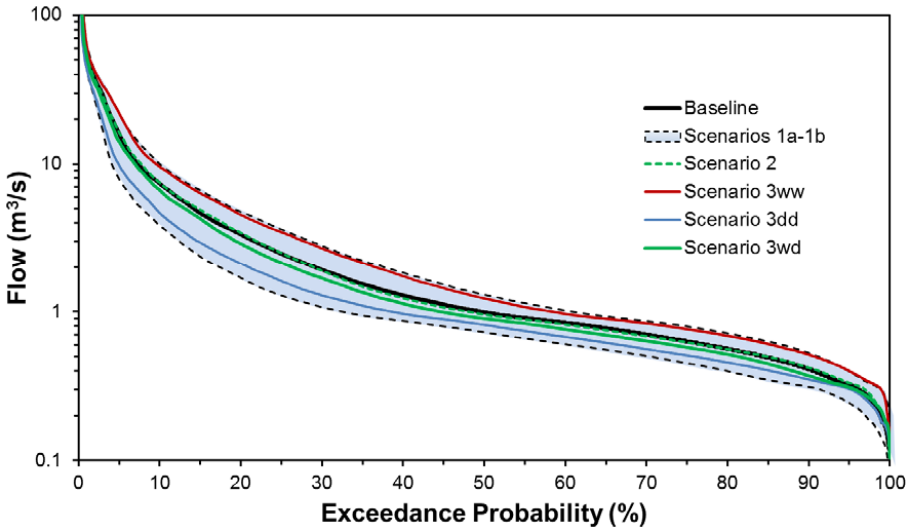

Figure 5. The streamflow exceedance probability curve for the Baseline and six future mid-21st century climate scenarios.

3.2. Analysis of Hydrologic Indexes

In addition to the impacts on seasonal and annual changes in streamflows, a more complete understanding of the impacts of seven future climate scenarios must consider the impacts on hydrologic indices. Nine indexes of hydrologic alteration were used to evaluate the intra-annual characteristics of mean flows, low flows, and floods based on analysis of daily streamflow produced by SWAT (Table 4). The Baseline (no-change) scenario indexes were used as comparison with the other future scenarios

Mean annual streamflow (Table 4) showed a similar increase for Scenarios 1a (24%) and 3ww (20%) and a similar decrease for Scenarios 1b (−33%) and 3dd (−29%), whereas Scenarios 2 and 3wd

showed little change from Baseline. These shifts tend to fall in line with the associated shifts in annual precipitation for the seven scenarios (Table 2). However, none of the other hydrologic indices showed relative shifts that were consistent with those of annual precipitation or mean annual streamflow.

Overall, low-flow pulse count and duration generally followed the pattern of annual precipitation for the seven scenarios, with greater annual precipitation corresponding to fewer low-flow pulses and shorter low-flow durations (Table 4). Only a couple, minor exceptions were notable. Scenario 3ww produced longer low-flow pulses (+8% relative to Baseline) than would have been expected from its greater annual flows (+20%). Also, Scenario 2 produced slightly more low-flow pulses (6.7) than Baseline (6.0) even though it had a slightly greater mean annual streamflow (4.6 m^3/s vs. 4.5 m^3/s). Both these differences result from the important impact of higher temperature and higher ET on reducing precipitation excess and producing less streamflow than would be expected based on changes in precipitation alone. The differences also suggest that seasonal variation in precipitation excess may be important in simulating low-flow responses to climate change scenarios.

The greatest magnitude and most variable impact of the climate scenarios was observed in changes to streamflow for both small flood (2-year return interval) and large flood (10-year return interval) peak, duration, and frequency (Table 4). Flood frequency for small floods was unchanged from Baseline for Scenarios 1a, 2, and 3ww and decreased for 3wd (−30%), 1b (−50%), and 3dd (−75%). Duration of small floods substantially increased from Baseline only for Scenario 1a (+20%) and decreased for Scenarios 3dd (−49%) and 1b (−52%).

The two substantially higher-flow scenarios (1a and 3ww) both produced fewer low-flow pulses than Baseline. But whereas 1a had an accompanying decrease in low-flow pulse duration (−16%), 3ww had longer low-flow pulse duration (+8%). This was accompanied by 3ww, having a slightly lower small-flood peak (−3%) and duration (−7%) and no change in frequency relative to Baseline. Interestingly, 3ww also had the greatest increase in large-flood peak magnitude (1294 m^3/s, +66%) but with shorter duration (−16%) and lower frequency (−60%) relative to Baseline. By comparison, 1a had only slight increases in small-flood (+2%) and large-flood (+8%) peaks, moderate increases in durations (+20%, +13%), and no change in frequency relative to Baseline. Also by comparison, the ensemble-mean Scenario 2 had relatively small changes (12% magnitude or less) from Baseline in annual flow as well as low-flow and flood-flow magnitudes, durations, and frequencies.

These results highlight a key difference between the 1a and 3ww scenarios. Although they had similar increases in mean annual flows, 3ww had fewer but longer periods of drought (low-flow pulses); relatively little change in frequency but shorter and less intense small floods; and dramatically fewer, shorter, and more intense large floods than Scenario 1a. The same comparison (fewer, longer droughts; shorter, less-intense small floods; fewer, shorter, more-intense large floods) holds when comparing 3ww to the ensemble-mean Scenario 2 or Baseline. This critical result demonstrates that hydrologic impacts of climate change scenarios must consider more than impacts on mean annual flows, but also impacts on other characteristics of low-flow and high-flow magnitudes, durations, and frequencies. It also demonstrates that simplified scenarios that assume stationary climatic conditions, such as Scenario 1a with a uniform 10% increase in precipitation based on historical precipitation patterns, do not capture the important impacts of changing climate evident in GCM results. In addition, these results demonstrate the importance of retaining seasonal variability of sets of GCM results with consistent patterns rather than blindly averaging all GCMs.

The two substantially lower-flow scenarios (3dd and 1b) both have more low-flow pulses with longer duration. Although both 3dd and 1b had large declines in small flood frequency and duration, 1b had an increase in small-flood peak (+5%) whereas 3dd had a decrease (−15%) relative to Baseline. Conversely for large floods, 3dd had a greater increase in peak (+25% relative to Baseline) than 1b (+6%), but with half the events and longer durations than 1b. Again, although mean annual-flow declines relative to Baseline were similar for 3dd and 1b, their low-flow and flood-flow responses had substantial differences. The 3dd scenario, based on an ensemble of a subset of GCM results, again showed greater changes to large-flood events than small-flood events.

4. Discussion

Although the results from the scenarios in group 1 demonstrated interaction between uniform monthly precipitation shifts and a general trend of temperature increase, overall the hydrologic response was predictable, for example, resulting in either an increase (Scenario 1a) or decrease (1b) in average daily streamflow for all months as well as hydrologic indexes in Table 4. While these simplified non-GCM-based scenarios are relevant for the studies on annual streamflow sensitivity to climate shifts, using them alone does not provide an adequate representation of hydrologic response to probable future scenarios. Hence, utilization of projections from GCMs is preferable to better portray possible future climate impacts on watershed hydrology.

GCMs simulate the non-stationary climatic effects on precipitation and temperature and provide useful projections for potential future climate. The use of an ensemble of GCMs, similar to scenario 2, avoids biases from a single GCM and provides an orchestrated perspective on potential climate changes, except for the cases of individual models specifically developed to account for unique global events. No GCM from the available pool of models was specifically calibrated for northeast Kansas; thus, the ensemble of GCMs would be expected to better represent a consensus of forcing data to assess future impacts on watershed hydrology at the local scale than the use of one specific model. The ensemble mean approach used in Scenario 2 produced streamflows higher in spring and lower in summer compared to Baseline, which was consistent with precipitation changes in these seasons. Even though annual total precipitation remained within the normal range of variation for this region, a shift toward higher precipitation in the earlier spring followed by higher probability of a drought in the summer caused substantial streamflow shifts that may be associated with adverse impacts on agricultural production and water resources. Although crops may have adequate or excessive precipitation and soil water in the early growing stages, water stress late in the summer may lead to increased irrigation demand or water-stressed dryland crops.

Three scenarios of Group 3 used subsets of the 15 GCMs to highlight three distinct seasonal trends, thus increasing the seasonal variability in precipitation projections compared to the use of the 15-model ensemble utilized in Scenario 2. The range of future climate trends in the Group 3 climate scenarios resulted in a wider range of hydrologic alteration. The projections of Group 3 scenarios produced an interesting situation for agricultural operations in northeast Kansas. With an increase in precipitation throughout the growing season (April–September) in Scenario 3ww, crops may become less dependent on irrigation input, which would reduce groundwater consumption and increase baseflow. Increased rainfall during the growing season may also provide an increase in crop yield. Aquatic ecosystems would experience a substantial shift in hydrologic regime from all three group 3 scenarios, with either less frequent (3ww) or more frequent (3wd, 3dd) but longer (3ww, 3wd, 3dd) low-flow periods and less frequent (3ww, 3dd) but higher intensity (3ww, 3wd, 3dd) large flood events. The higher-intensity runoff events would also increase erosion, especially if they occur in early spring when many agricultural fields are bare or have low residue cover, causing land management concerns as well as increased sediment in streams and reservoirs. Scenarios 3ww, 3wd, and 2 all caused higher rates of runoff to shift into earlier times of the year when ground cover on agricultural fields in northeast Kansas is at a minimum, thus resulting in an increase in runoff and erosion during the early part of the year. The same factors that led to longer low-flow pulses for all group 3 scenarios and greater number of low-flow pulses for 3wd and 3dd would also create the need for increased irrigation.

While it is unlikely that the climate scenarios generated for this study area would be the same for other areas, the methods used to generate these climate scenarios and create locally relevant subsets of GCM climate projections can be used to generate future scenarios for any watershed around the world. The resultant climate scenarios from both Groups 2 and 3 development procedures are better for analysis because they do not rely on a single GCM projection, but the seasonal variability of projected climate captured in the group 3 scenarios provides a greater range of potential hydrologic impacts from climate change and provides a more robust set of scenarios for water planners and managers to constrain future decisions.

5. Conclusions

An analysis of climate projections, including a continuation of baseline historical climate, stationary climate shifts of 10% greater or less precipitation than baseline, and non-stationary shifts created using various ensembles of 15 GCMs, was conducted for the mid-21st century (2046−2065) high-emission A2 scenario and applied to SWAT model built for Soldier Creek watershed in northeast Kansas. Daily timeseries of precipitation and minimum and maximum temperature were developed with the stochastic weather generator WINDS and bias-corrected on the historical temperature and precipitation data collected from 1960 to 1990 at the Topeka airport weather station. Analysis of annual, monthly, and daily streamflow statistics were conducted for baseline and six future climate scenarios and alterations of hydrologic regimes from the baseline scenario was documented.

The results of the study can be summarized as the following.

- The use of stationary uniform shifts of ±10% of historical precipitation provided a reasonable bound of maximum and minimum annual and seasonal hydrological response to projected future climate, but they did not capture important shifts in drought and flood behaviors of streamflow.
- The use of an ensemble mean of 15 GCMs was found to be an efficient way to capture the non-stationary effects of projected future climate without the bias generated by assumptions and specifics of an individual GCM, but it also did not capture important shifts in drought and flood behaviors of streamflow.
- The new approach that used seasonally-consistent subset ensembles of the 15 GCMs highlighted a range of distinct seasonal streamflow trends and hydrological responses not captured by non-stationary or full-ensemble approaches.
- Using subsets of seasonally-consistent GCMs was extremely important in considering ranges of hydrologic impacts of future climate projections, particularly for the extreme low-flow and high-flow event magnitude, frequency, and duration.
- The use of a stochastic weather generator (WINDS) in generating daily climate variables simulated daily storms based on the precipitation probability distribution inherited from the validation record and provided an efficient and reproducible method of downscaling monthly GCM data for daily hydrological model input.
- The methods used to develop the scenarios and subset ensembles can be universally applied to any region.

Acknowledgments: The authors thank Chris Siebenmorgen for assisting with watershed model simulations. This material is based on work supported by the USDA Hatch Project No. S-1063, the NSF-CNH Program (award number 1313815), and the Kansas Agricultural Experiment Station, Manhattan, Kan., Contribution No. 17-357-J.

Author Contributions: Aleksey Y. Sheshukov and Kyle R. Douglas-Mankin conceived and designed the experiments, performed the simulations, analyzed the data, and wrote the paper.

Conflicts of Interest: The authors declare no conflict of interest.

References

1. IPCC-DDC Data Distribution Center. Available online: http://ipcc-data.org/ (accessed on 16 March 2017).
2. Intergovernmental Panel on Climate Change Fourth Assessment Report Working Group I (IPCC AR4 WG1). Climate Change 2007: The Physical Science Basis. In *Contribution of Working Group I to the Fourth Assessment Report of the Intergovernmental Panel on Climate Change*; Solomon, S., Qin, D., Manning, M., Chen, Z., Marquis, M., Averyt, K.B., Tignor, M., Miller, H., Eds.; Cambridge University Press: Cambridge, UK, 2007.
3. Chen, J.; Brissette, F.P.; Poulin, A.; Leconte, R. Overall uncertainty study of the hydrological impacts of climate change for a Canadian watershed. *Water Resour. Res.* **2011**, *47*, W12509. [CrossRef]
4. Kay, A.; Davies, H.; Bell, V.; Jones, R. Comparison of uncertainty sources for climate change impacts: Flood frequency in England. *Clim. Chang.* **2009**, *92*, 41–63. [CrossRef]
5. Wilby, R.; Harris, I. A framework for assessing uncertainties in climate change impacts: Low-flow scenarios for the River Thames, UK. *Water Resour. Res.* **2006**, *42*, W02419. [CrossRef]

6. Maraun, D.; Wetterhall, F.; Ireson, A. Precipitation downscaling under climate change: Recent developments to bridge the gap between dynamical models and the end user. *Rev. Geophys.* **2010**, *48*. [CrossRef]
7. Chen, J.; Brissette, F.P.; Leconte, R. Assessing regression-based statistical approaches for downscaling precipitation over North America. *Hydrol. Process.* **2014**, *28*, 3482–3504. [CrossRef]
8. Feddersen, H.; Andersen, U. A method for statistical downscaling of seasonal ensemble predictions. *Tellus A* **2005**, *57*, 398–408. [CrossRef]
9. Sharma, D.; Gupta, A.; Babel, M. Spatial disaggregation of bias-corrected GCM precipitation for improved hydrologic simulation: Ping River Basin, Thailand. *Hydrol. Earth* **2007**, *11*, 1373–1390. [CrossRef]
10. Wilby, R.; Hay, L.; Leavesley, G. A comparison of downscaled and raw GCM output: Implications for climate change scenarios in the San Juan River basin, Colorado. *J. Hydrol.* **1999**, *225*, 67–91. [CrossRef]
11. Sheshukov, A.Y.; Siebenmorgen, C.B.; Douglas-Mankin, K.R. Seasonal and annual impacts of climate change on watershed response using an ensemble of global climate models. *Trans. ASABE* **2011**, *54*, 2209–2218. [CrossRef]
12. Fowler, H.J.; Blenkinsop, S.; Tebaldi, C. Linking climate change modelling to impacts studies: Recent advances in downscaling techniques for hydrological modelling. *Int. J. Climatol.* **2007**, *27*, 1547–1578. [CrossRef]
13. Zhang, X.-C.; Nearing, M.A.; Garbrecht, J.D.; Steiner, J.L. Downscaling Monthly Forecasts to Simulate Impacts of Climate Change on Soil Erosion and Wheat Production. *Soil Sci. Soc. Am. J.* **2004**, *68*, 1376–1385. [CrossRef]
14. Zhang, Y.G.; Nearing, M.A.; Zhang, X.C.; Xie, Y.; Wei, H. Projected rainfall erosivity changes under climate change from multimodel and multiscenario projections in Northeast China. *J. Hydrol.* **2010**, *384*, 97–106. [CrossRef]
15. Zhang, X.C.; Nearing, M.A. Impact of climate change on soil erosion, runoff, and wheat productivity in central Oklahoma. *Catena* **2005**, *61*, 185–195. [CrossRef]
16. Jha, M.; Arnold, J.; Gassman, P. Climate chhange sensitivity assessment on upper mississippi river basin streamflows using SWAT. *J. Am. Water Resour. Assoc.* **2006**, *42*, 997–1015. [CrossRef]
17. Siebenmorgen, C.B.; Sheshukov, A.Y.; Douglas-Mankin, K.R. Impacts of climate change on hydrologic indices in a Northeast Kansas watershed. In Proceedings of the 5th Conference on Watershed Management to Improve Water Quality (TMDLs), Baltimore, MD, USA, 14–17 November 2010; American Society of Agricultural and Biological Engineer (ASABE): St. Joseph, MI, USA, 2010.
18. Zhang, X.-C. A comparison of explicit and implicit spatial downscaling of GCM output for soil erosion and crop production assessments. *Clim. Chang.* **2007**, *84*, 337–363. [CrossRef]
19. Githui, F.; Gitau, W.; Mutua, F.; Bauwens, W. Climate change impact on SWAT simulated streamflow in western Kenya. *Int. J. Climatol.* **2009**, *29*, 1823–1834. [CrossRef]
20. Chaubey, I.; Bosch, D.; Muñoz-Carpena, R.; Harmel, R.D.; Douglas-Mankin, K.R.; Nejadhashemi, A.; Srivastava, P.; Shirmohammadi, A. Climate Change: A Call for Adaptation and Mitigation Strategies. *Trans. ASABE* **2016**, *59*, 1709–1713.
21. Aumen, N.; Havens, K.; Best, G.; Berry, L. Predicting ecological responses of the Florida Everglades to possible future climate scenarios: Introduction. *Environ. Manag.* **2015**, *55*, 741–748. [CrossRef] [PubMed]
22. Brunsell, N.A.; Jones, A.R.; Jackson, T.L.; Feddema, J.J. Seasonal trends in air temperature and precipitation in IPCC AR4 GCM output for Kansas, USA: Evaluation and implications. *Int. J. Climatol.* **2010**, *30*, 1178–1193. [CrossRef]
23. Karl, T.R.; Melillo, J.M.; Peterson, T.C. *Global Climate Change Impacts in the United States*; Cambridge University Press: New York, NY, USA, 2009.
24. Juracek, K. *Historical Channel Change Along Soldier Creek, Northeast Kansas*; USGS Water-Resources Investigations Report 02-4047; United States Geological Survey: Reston, VA, USA, 2002.
25. United States Geological Survey (USGS). *The National Map*; USGS: Reston, VA, USA, 2016.
26. Arnold, J.; Srinivasan, R.; Muttiah, R.; Williams, J. Large area hydrologic modeling and assessment part I: Model development. *J. Am. Water Resour. Assoc.* **1998**, *34*, 73–89. [CrossRef]
27. Neitsch, S.; Arnold, J.; Kiniry, J.; Williams, J. *Soil and Water Assessment Tool Theoretical Documentation*; Version 2009; Texas Water Resources Institute: College Station, TX, USA, 2011.

28. Arnold, J.G.; Youssef, M.A.; Yen, H.; White, M.J.; Sheshukov, A.Y.; Sadeghi, A.M.; Moriasi, D.N.; Steiner, J.L.; Amatya, D.M.; Skaggs, R.W.; et al. Hydrological Processes and Model Representation: Impact of Soft Data on Calibration. *Trans. ASABE* **2015**, *58*, 1650–1660.
29. Douglas-Mankin, K.; Srinivasan, R.; Arnold, J. Soil and Water Assessment Tool (SWAT) model: Current developments and applications. *Trans. ASABE* **2010**, *53*, 1423–1431. [CrossRef]
30. Gassman, P.; Reyes, M.; Green, C.; Arnold, J. The Soil and Water Assessment Tool: Historical Development, Applications, and Future Research Directions. *Trans. ASABE* **2007**, *50*, 1211–1240. [CrossRef]
31. Gassman, P.; Sadeghi, A.; Srinivasan, R. Applications of the SWAT model special section: Overview and insights. *J. Environ. Qual.* **2014**, *43*, 1–8. [CrossRef] [PubMed]
32. Tuppad, P.; Douglas-Mankin, K.; Lee, T.; Srinivasan, R.; Arnold, J.G. Soil and Water Assessment Tool (SWAT) Hydrologic/Water Quality Model: Extended Capability and Wider Adoption. *Trans. ASABE* **2011**, *54*, 1677–1684. [CrossRef]
33. USDA-NRCS Geospatial Data Gateway. Available online: https://gdg.sc.egov.usda.gov/ (accessed on 1 January 2016).
34. Homer, C.; Huang, C.; Yang, L.; Wylie, B. Development of a 2001 national land-cover database for the United States. *Photogramm. Eng. Remote Sens.* **2004**, *70*, 829–840. [CrossRef]
35. WRAPS Delaware River Watershed Restoration and Protection Strategy. Nine Element Watershed Plan Summary. Available online: http://www.kswraps.org/files/attachments/delaware_plansummary.pdf (accessed on 1 January 2016).
36. NOAA-NCEI Climate-radar Data Inventories. Available online: https://www.ncdc.noaa.gov/ (accessed on 1 January 2016).
37. Moriasi, D.; Arnold, J.; Van Liew, M.; Bingner, R.; Harmel, R.; Veith, T. Model evaluation guidelines for systematic quantification of accuracy in watershed simulations. *Trans. ASABE* **2007**, *50*, 885–900. [CrossRef]
38. Siebenmorgen, C.B. *Potential Climate Change Impacts on Hydrologic Regimes in Northeast Kansas*; Kansas State University: Manhattan, KS, USA, 2010.
39. Indicators of Hydrologic Alteration (IHA). *Indicators of Hydrologic Alteration User's Manual*; Ver. 7.1; IHA: Arlington, VA, USA, 2009.
40. Wilson, B.N.; Sheshukov, A.Y.; Pulley, R. Chapter 3: Modeling algorithms of the WINDS model. In *Erosion Risk Assessment Tool for Construction Sites*; Research Report No. MN/RC-2006-27; Wilson, B., Sheshukov, A., Pulley, R., Eds.; Minnesota Department of Transportation: St. Paul, MN, USA, 2006.
41. Richardson, C. Stochastic simulation of daily precipitation, temperature, and solar radiation. *Water Resour. Res.* **1981**, *96*, 85–101. [CrossRef]
42. Wilson, B.N.; Sheshukov, A.Y. Precipitation parameters of stochastic climate models for a changing climate. In Proceedings of the International Symposium on Erosion and Landscape Evolution (ASABE), Anchorage, AK, USA, 18–21 September 2011.
43. Chen, J.; Brissette, F.P. Combining Stochastic Weather Generation and Ensemble Weather Forecasts for Short-Term Streamflow Prediction. *Water Resour. Manag.* **2015**, *29*, 3329–3342. [CrossRef]
44. Teutschbein, C.; Seibert, J. Regional Climate Models for Hydrological Impact Studies at the Catchment Scale: A Review of Recent Modeling Strategies. *Geogr. Compass* **2010**, *4*, 834–860. [CrossRef]
45. Gao, J.; Sheshukov, A.Y. Uncertainty Estimation of Hydrological Impacts of Bias-Corrected CMIP5 Climate Change Projections. In Proceedings of the International Soil and Water Assessment Tool Conference, West Lafayette, IN, USA, 14–16 October 2015.
46. Dodds, W.K.; Gido, K.; Whiles, M.R.; Fritz, K.M.; Matthews, W.J. Life on the Edge: The Ecology of Great Plains Prairie Streams. *Bioscience* **2004**, *54*, 205. [CrossRef]